The EMBO Journal vol.13 no.9 pp.2056–2065, 1994

Complex asparagine-linked oligosaccharides are required for morphogenic events during post-implantation development

Martina Metzler[1], Anita Gertz[1], Mohan Sarkar[5], Harry Schachter[5], John W.Schrader[1,4] and Jamey D.Marth[1,2,3,6]

[1]The Biomedical Research Centre and the Departments of [2]Medical Genetics, [3]Biochemistry and [4]Medicine, 2222 Health Sciences Mall, University of British Columbia, Vancouver, British Columbia, V6T 1Z3 and [5]Department of Biochemistry, Hospital for Sick Children and the University of Toronto, Toronto, Ontario, M5G 1X8, Canada
[6]Corresponding author

Communicated by R.Dwek

Complex asparagine (N)-linked oligosaccharides appear late in phylogeny and are highly regulated in vertebrates. Variations in these structures are found on the majority of cell-surface and secreted proteins. Complex N-linked oligosaccharide biosynthesis is initiated in the Golgi apparatus by the action of *Mgat-1*-encoded UDP-*N*-acetylglucosamine:α-3-D-mannoside β-1,2-*N*-acetylglucosaminyltransferase I (GlcNAc-TI). To determine if these structures govern ontogenic processes in mammals, mouse embryos were generated that lacked a functional *Mgat-1* gene. Inactivation of both *Mgat-1* alleles produced deficiencies in GlcNAc-TI activity and complex N-linked oligosaccharides. Embryonic lethality occurred by day 10.5, thus establishing that complex N-linked oligosaccharides are required during post-implantation development. Remarkably, embryonic development proceeded into day 9 with the differentiation of multiple cell types. Complex N-linked oligosaccharides are important for morphogenic processes as neural tube formation, vascularization and the determination of left–right body plan asymmetry were impaired in the absence of a functional *Mgat-1* gene.

Key words: gene targeting/mammalian ontogeny/N-linked oligosaccharides

Introduction

Mammalian organisms generate an abundant and diverse repertoire of oligosaccharide structures, including those that are linked to asparagine (N-linked), or serine and threonine (O-linked) residues on proteins (for review, see Varki, 1993; Fukuda, 1992). N- and O-linked oligosaccharides are expressed on the majority of cell surface and secreted proteins and their synthesis is highly regulated during differentiation and growth as well as in inflammation, neoplasia and metastasis (Dennis *et al.*, 1987; Bolscher *et al.*, 1988; Passaniti and Hart, 1990; Fernandes *et al.*, 1991). Experiments with glycosylation inhibitors, glycosidases and mutant cell lines indicate that some proteins require modification by specific oligosaccharides for normal function *in vitro* (for review, see Varki, 1993). Moreover, cell–cell adhesion *in vivo* can depend upon specific oligosaccharide structures, as exemplified in studies on the mechanism of hemopoietic cell interaction with vascular endothelium during inflammatory responses (for review, see Lasky, 1992).

Complex (including hybrid) N-linked oligosaccharide structures display remarkable diversity due to variations in the saccharide units transferred and the glycosidic linkages formed (Kornfeld and Kornfeld, 1985). Such diversity is controlled by the regulated expression of specific glycosyltransferases that display remarkable substrate specificity for pre-existing oligosaccharide structures (for review, see Paulson and Colley, 1989; Schachter *et al.*, 1989). Moreover, the biosynthesis of complex N-linked oligosaccharide structures has been clarified as crucial steps in the protein glycosylation pathway have been reconstructed *in vitro* following the characterization and cloning of specific glycosyltransferases. *In vivo*, the biosynthetic pathway is initiated in the endoplasmic reticulum (ER) with the transfer of the oligo-mannose precursor to specific asparagine residues in a co-translational process. Following processing in the ER and the *cis* Golgi cisternae, the stepwise covalent linkage of specific saccharide units to the processed high-mannose core generates complex N-linked oligosaccharides (Figure 1).

UDP-*N*-acetylglucosamine:α-3-D-mannoside β-1,2-*N*-acetylglucosaminyltransferase I (EC 2.4.1.101; GlcNAc-TI) is a key enzyme in N-linked protein glycosylation since its action in the medial compartment of the Golgi apparatus is essential for subsequent glycosylation steps that convert the processed high-mannose core into complex N-linked oligosaccharide structures (Figure 1). In the absence of GlcNAc-TI activity, N-linked carbohydrate addition is limited to the production of the high-mannose structure. Interestingly, complex N-linked oligosaccharides do not appear to be required for mammalian cell viability *in vitro*. The Lec-1 derivative of the Chinese hamster ovary cell line proliferates and functions normally, although this subline is incapable of generating complex N-linked oligosaccharide structures due to a mutagenic loss of GlcNAc-TI activity (Stanley *et al.*, 1975; Kumar and Stanley, 1989). Nevertheless, the amino acid sequence of GlcNAc-TI is highly conserved among mammals and is encoded by a single gene locus termed *Mgat-1* in the mouse (Kumar *et al.*, 1990; Sarkar *et al.*, 1991; Pownall *et al.*, 1992). *Mgat-1* RNA expression has been detected in all mouse tissues analyzed thus far (Kumar *et al.*, 1992; Pownall *et al.*, 1992).

In contrast to higher eukaryotes, some multicellular organisms, including fungi, do not synthesize complex N-linked oligosaccharides and instead display the processed high-mannose core (for review, see Kukuruzinska *et al.*, 1987; Tanner and Lehle, 1987). To investigate the possible ontogenic roles of complex N-linked oligosaccharides in mammalian development, mouse embryos were generated

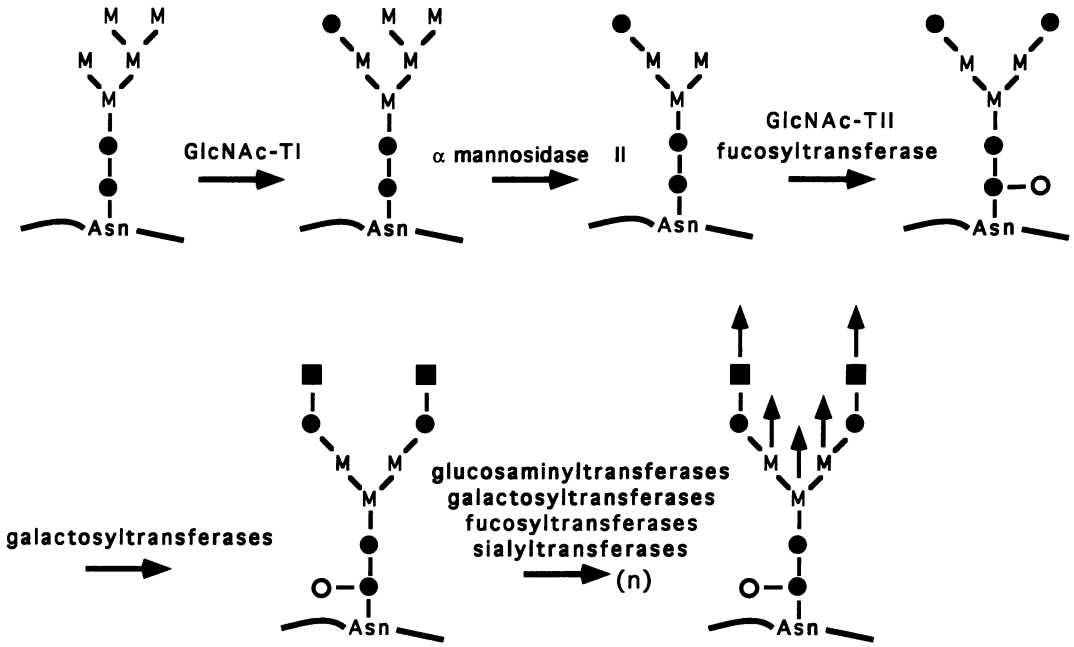

Fig. 1. *Mgat-1*-encoded GlcNAc-TI regulates complex N-linked oligosaccharide addition to the processed high-mannose core. Following processing of the oligo-mannose complex that is added to asparagine residues in the endoplasmic reticulum, the high-mannose core (top left) acts as the specific substrate for the initiation of complex structures by the action of GlcNAc-TI in the medial Golgi (Kornfeld and Kornfeld, 1985). Carbohydrate residues depicted include those derived from glucosamine (closed circle), mannose (M), fucose (open circle) and galactose (closed square). Additional variations and branches can occur and are represented by the four vertical arrows.

that lacked a functional *Mgat-1* gene following homologous recombination in embryonic stem cells. The results presented herein reveal that complex N-linked oligosaccharides provide vital information that is required during mouse embryogenesis.

Results

Mgat-1 mutagenesis in embryonic stem cells and generation of Mgat-1$^+$/Mgat-1$^-$ mice

Mgat-1 genomic DNA was mutagenized in embryonic stem (ES) cells by inserting a neomycin phosphotransferase expression cassette (pMC1neopolyA) into the single protein-encoding exon (Figure 2A). The pMC1neopolyA cistron is flanked by 2.4 kb and 0.8 kb of *Mgat-1* sequence. Following electroporation of the *Mgat-1* targeting construct into the D3 ES cell line, homologous recombinants were detected at a frequency of 1/120 G418-resistant clones by polymerase chain reaction (PCR). These were confirmed by genomic Southern blotting analyses (Figure 2B, left). Microinjection of *Mgat-1*-targeted ES cells into C57BL/6 pre-implantation embryos resulted in germline colonization in chimeric mice. Offspring that were heterozygous for the mutation at the *Mgat-1* locus were identified by genomic Southern blotting analyses (see below).

Homozygous mutation at the Mgat-1 locus is lethal during embryogenesis

Analyses of *Mgat-1* genomic DNA from over 85 offspring derived from matings between heterozygous *Mgat-1* mutant mice revealed that only wild-type (*Mgat-1$^+$/Mgat-1$^+$*) or heterozygous (*Mgat-1$^+$/Mgat-1$^-$*) mice were born, at a ratio of 1:2, respectively (Figure 2B, right). These results implied that *Mgat-1$^-$/Mgat-1$^-$* embryos died prior to birth.

To determine the developmental stage at which *Mgat-1$^-$/Mgat-1$^-$* embryos die, development was monitored following timed matings of *Mgat-1$^+$/Mgat-1$^-$* mice. Although some oligosaccharide structures appear critical during pre-implantation (Bayna *et al.*, 1988; Muramatsu, 1988; Varki *et al.*, 1991), *Mgat-1$^-$/Mgat-1$^-$* embryos developed normally to the blastocyst stage upon culture of fertilized oocytes (data not shown). However, during post-implantation development, a significant number of intra-uterine resorption sites were observed at embryonic day 10.5 (E10.5). DNA was isolated from embryonic tissues of E10.5 embryos and assessed for *Mgat-1* genomic structure. The *Mgat-1$^-$/Mgat-1$^-$* genotype was invariably found in these resorption sites indicating that the *Mgat-1$^-$/Mgat-1$^-$* genotype is lethal by approximately E10.5 (data not shown). The latest time-point wherein all embryos were viable appeared to be E9.5. Of 242 E9.5 embryos analyzed by PCR and Southern blotting, 24% were *Mgat-1$^+$/Mgat-1$^+$*, 53% were *Mgat-1$^+$/Mgat-1$^-$* and 23% were *Mgat-1$^-$/Mgat-1$^-$*, as expected for a normal Mendelian distribution (Figure 2C and data not shown).

Loss of GlcNAc-TI activity and complex N-linked oligosaccharides in Mgat-1$^-$/Mgat-1$^-$ embryos

Specific measurements of GlcNAc-T1 activity can be obtained using Manα1-6(Manα1-3)Manβ-octyl [Man_3-$C_{(8)}$] or the ovalbumin derived peptide [Manα1-6(Manα1-3)Manα1-6](Manα1-3)Manβ1-4GlcNAcβ1-4GlcNAc-Asn (Man_5-Asn) as substrate (Vella *et al.*, 1984; Palcic *et al.*, 1988). GlcNAc-T1 specific activity was quantitated in cellular extracts derived from whole embryos at E9.5. Using Man_3-$C_{(8)}$ as a substitute, embryos that harbored a functional *Mgat-1* gene at both alleles exhibited GlcNAc-TI activity that measured 0.70 nmol/mg/h (Table I). This value

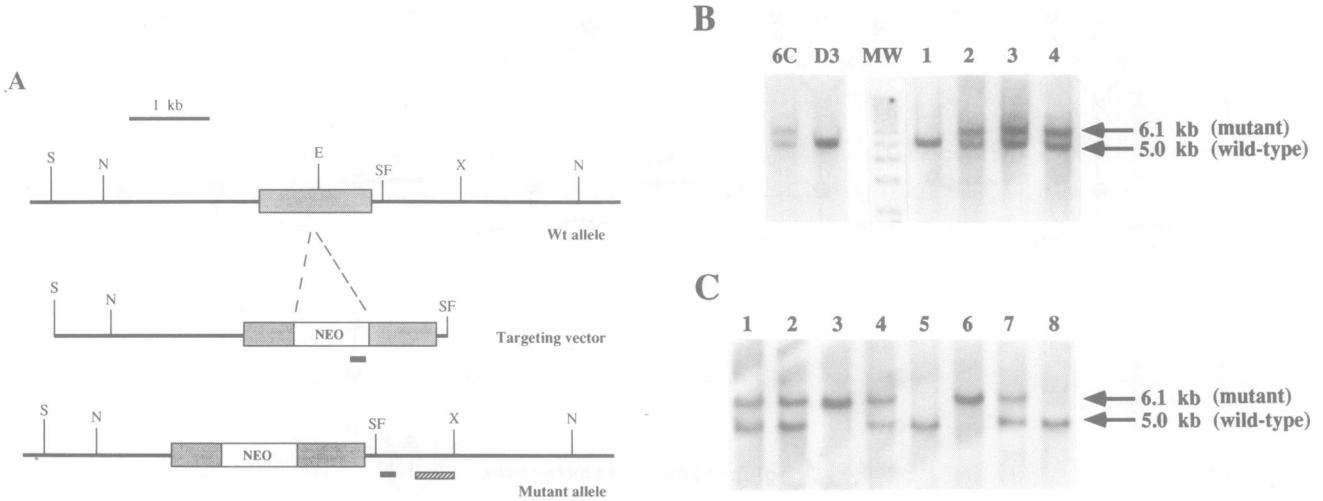

Fig. 2. *Mgat-1* mutation as established in the germline of mice. (**A**) Diagram of the wild-type *Mgat-1* allele, the targeting construct and the mutagenized *Mgat-1* allele. *Mgat-1* genomic sequences flank the single *Mgat-1* protein-encoding exon (boxed). The site of insertion of the neomycin phosphotransferase (Neo) expression cassette (*Eag*I site) is depicted. PCR primers are presented as short solid lines. The short stippled box represents the DNA probe used for Southern analyses. S, *Sac*I; N, *Nsi*I; E, *Eag*I; SF, *Sfi*I; X, *Xho*I. (**B**, left) Genomic *Mgat-1* structure in D3 ES cell clone 6C that has undergone homologous recombination as compared with parental D3 ES cells. (**B**, lanes 1–5) *Mgat-1* structure in newborn mice derived from matings of *Mgat-1*$^+$/*Mgat-1*$^-$ mice. (**C**) Genomic *Mgat-1* Southern analyses of DNA isolated from cultured primary embryonic fibroblasts derived from disaggregated E9.5 embryos. For Southern blotting 5 μg of genomic DNA was digested with *Nsi*I. Molecular weights are determined by comparison with DNA markers (MW).

Table I. Embryonic GlcNAc-TI activity and complex N-linked oligosaccharide abundance

Genotype	*Mgat-1*$^+$/*Mgat-1*$^+$	*Mgat-1*$^+$/*Mgat-1*$^-$	*Mgat-1*$^-$/*Mgat-1*$^-$
GlcNAc-TI activity	0.70	0.38	<0.04
High-mannose/complex N-linked oligosaccharides	2.3	4.8	15.8

GlcNAc-TI specific activity was determined by measuring the ability of E9.5 embryo extracts to catalyze the transfer of *N*-[^{14}C]acetyl-D-glucosamine from UDP-*N*-[^{14}C]acetyl-D-glucosamine to Manα1-6(Manα1-3)Manβ-octyl. Values are given in nmol transferred/mg embryo protein per hour. The ratio of high-mannose to complex N-linked oligosaccharides is depicted following quantitation of ConA and ricin binding to [^{3}H]glycopeptides derived from E9.5 embryo extracts. Assays were done in duplicate with standard deviations < 10% of indicated values.

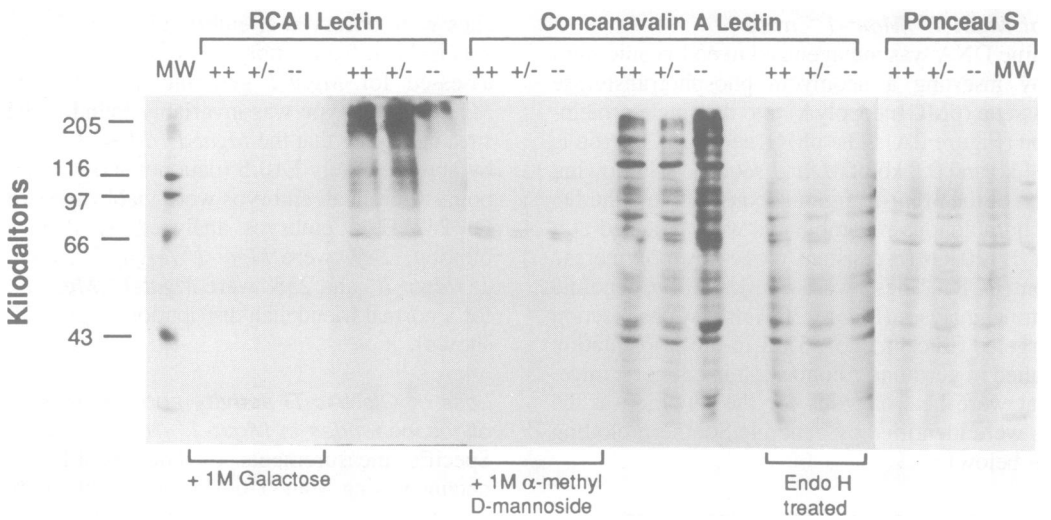

Fig. 3. *Mgat-1*$^-$/*Mgat-1*$^-$ embryos harbor increased levels of high-mannose structures on many glycoproteins while complex N-linked oligosaccharides are depleted. Extracts derived from wild-type (++), heterozygous (+/−), and *Mgat-1*$^-$/*Mgat-1*$^-$ (−−) mouse embryos, corresponding to 22.5 μg of protein, were electrophoresed on 10% SDS–polyacrylamide mini-gels and blotted to nitrocellulose. After staining with Ponceau S, filters were incubated with either biotinylated *Ricinis communis* agglutinin I lectin (RCA I), or biotinylated ConA in the presence or absence of 1 M galactose or 1 M α-methyl D-mannoside, respectively. Bound lectins and biotinylated molecular weight standard proteins (MW) were detected using ECL (Amersham). As shown, lectin binding was absent in the presence of the correponding competitive sugar. Furthermore, there was reduced ConA reactivity following endoglycosidase H (Endo H) treatment of embryo extracts, thereby confirming the specificity of this lectin reaction with high-mannose structures.

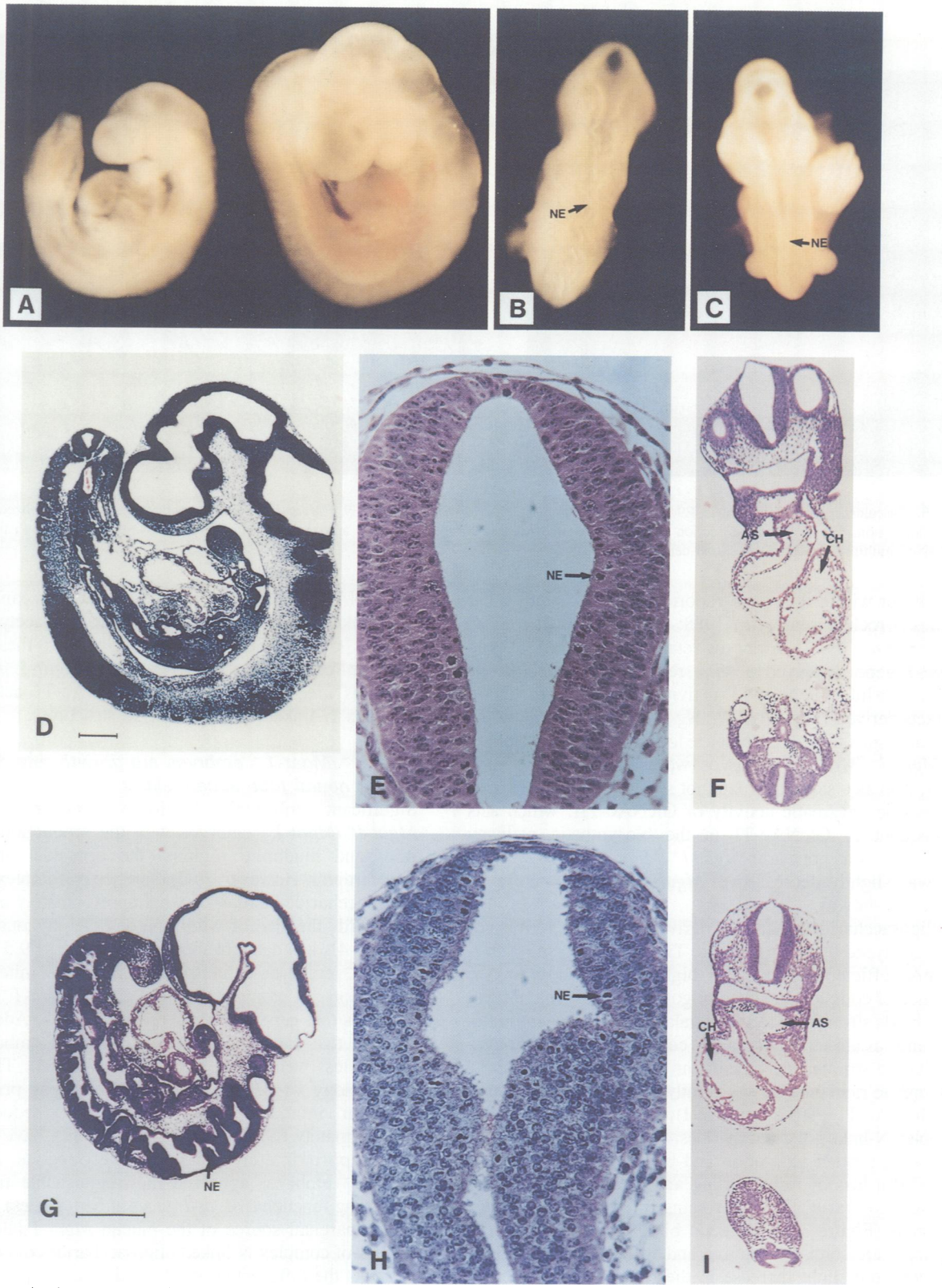

Fig. 4. Embryonic phenotypes resulting from loss of complex N-linked oligosaccharides. Whole embryos were visualized by light microscopy in (**A–C**). An *Mgat-1*$^{-}$*/Mgat-1*$^{-}$ embryo (A, left), harboring 20 somites, is compared with an *Mgat-1*$^{+}$*/Mgat-1*$^{+}$ embryo (A, right) with 26 somites isolated from the same female at E9.5. (B and C) Dorsal views of an E9.5 *Mgat-1*$^{-}$*/Mgat-1*$^{-}$ embryo and an E9.0 *Mgat-1*$^{+}$*/Mgat-1*$^{+}$ embryo both harboring 20 somites. A convoluted neural tube with a staggered suture line is present in the *Mgat-1*$^{-}$*/Mgat-1*$^{-}$ embryo. In (**D–I**), hematoxylin–eosin staining was performed on thin sections from (D–F) an E9.5 *Mgat-1*$^{+}$*/Mgat-1*$^{+}$ embryo and (G–I) an E9.5 *Mgat-1*$^{-}$*/Mgat-1*$^{-}$ embryo isolated from the same female. Longitudinal sections (D and G) reveal convoluted neural epithelium in the *Mgat-1*$^{-}$*/Mgat-1*$^{-}$ embryo (NE, arrow). The transverse sections (E and H) taken from the mid-trunk region show increased numbers of mitotic figures in neural epithelial cells in the *Mgat-1*$^{-}$*/Mgat-1*$^{-}$ embryo. Transverse sections (F and I) at the levels of otic vesicle and second branchial arch reveal a *situs inversus* phenotype in the *Mgat-1*$^{-}$*/Mgat-1*$^{-}$ embryo with inverted tail position and heart structure. NE, neural epithelium; CH, commom ventricular chamber of the heart; AS, aortic sac. The solid bar corresponds to a distance of 0.1 mm.

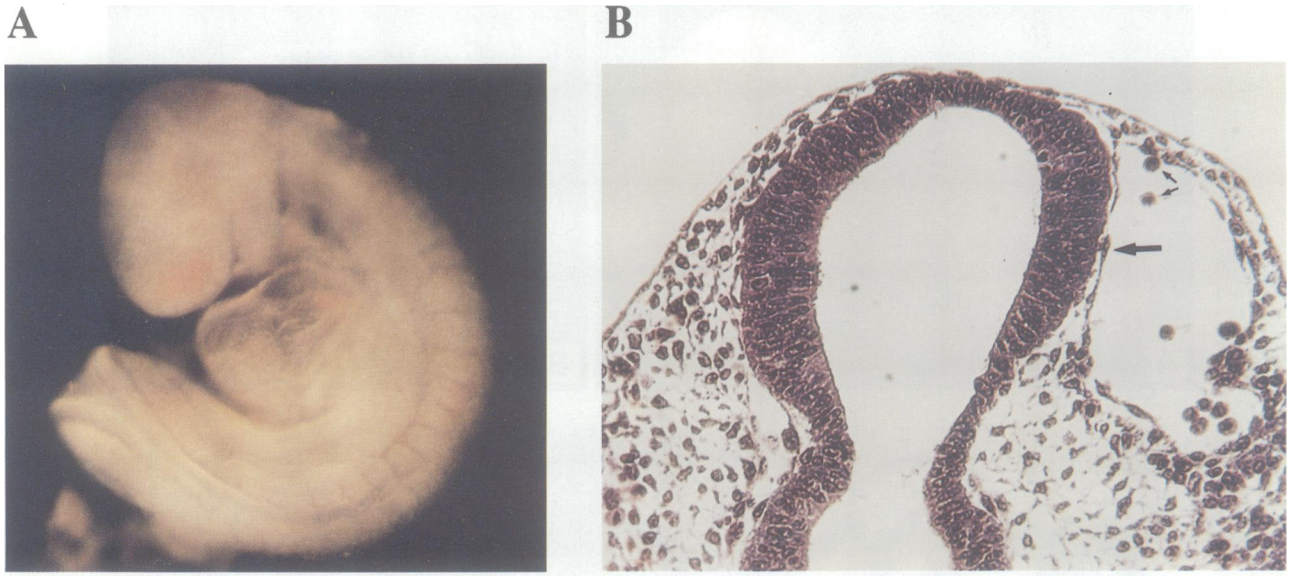

Fig. 5. Vascularization is impaired in E9.5 embryos lacking GlcNAc-TI activity. (**A**) E9.5 *Mgat-1*$^{-}$*/Mgat-1*$^{-}$ embryo displaying localized redness in the head region. (**B**) A transverse section from the fore- and mid-brain region revealed an expanded endothelial cell vasculature (arrow) that contained multiple nucleated red blood cells (small arrows).

is low but within the range reported among various adult tissues (Brockhausen *et al.*, 1988; Nishikawa *et al.*, 1988; Möller *et al.*, 1992). Embryos retaining a single wild-type *Mgat-1* gene displayed a 47% reduction in GlcNAc-T1 activity, while GlcNAc-T1 activity was not detected in extracts derived from *Mgat-1*$^{-}$*/Mgat-1*$^{-}$ embryos (Table I). Similar results regarding complete loss of GlcNAc-TI activity in *Mgat-1*$^{-}$*/Mgat-1*$^{-}$ embryos were also obtained using Man_5-Asn as a substrate (data not shown). In other experiments, the enyzmatic activity of GlcNAc-TII, which acts subsequent to GlcNAc-TI in the biosynthetic pathway (Figure 1), was normal in *Mgat-1*$^{+}$*/Mgat-1*$^{-}$ heterozygotes yet was slightly decreased in *Mgat-1*$^{-}$*/Mgat-1*$^{-}$ embryos (data not shown).

Oligosaccharide structures derived from E9.5 embryos were analyzed by lectin binding. The lectin concanavalin A (ConA) efficiently binds the high-mannose core in the absence of complex N-linked oligosaccharides. In contrast, ricin binds strongly to terminal galactose residues in asialo-tri- and asialo-tetra-antennary complex N-linked oligosaccharide structures (Narasimhan *et al.*, 1986). The ratio of ConA to ricin binding was greatly increased in the absence of GlcNAc-TI activity (Table I), reflecting the loss of complex N-linked oligosaccharides. Moreover, lectin binding following protein separation and blotting to nitrocellulose revealed a loss of ricin binding and an increase in ConA binding to various glycoproteins in *Mgat-1*$^{-}$*/Mgat-1*$^{-}$ embryos (Figure 3). The lectin binding results shown in Figure 3 are semi-quantitative and would not be expected to detect the slight increase in the ratio of ConA to ricin binding suggested in Table I for *Mgat-1*$^{+}$*/Mgat-1*$^{-}$ heterozygotes. Additionally, L-phytohemagglutinin (L-PHA), which binds to the Galβ1-4GlcNAcβ1-2(Galβ1-4GlcNAcβ1-6)-Manα portion of complex N-linked oligosaccharides (Narasimhan *et al.* 1986; Bierhuizen *et al.* 1988), failed to bind to *Mgat-1*$^{-}$*/Mgat-1*$^{-}$ embryonic tissues and did not aggregate single cells derived from yolk sac tissue (data not shown and see below). Low level ricin binding in the absence of GlcNAc-TI activity may indicate that ricin can also bind to O-linked oligosaccharides that contain *N*-acetylgalactosamine [GalNAc-Ser(Thr)]. Nevertheless, these results provide conclusive evidence that *Mgat-1*$^{-}$*/Mgat-1*$^{-}$ embryos are deficient in both GlcNAc-TI activity and complex N-linked oligosaccharide structures.

Mgat-1^{-}*/Mgat-1*$^{-}$ *embryos are growth retarded and exhibit neural tube abnormalities*

Significant embryonic development occurred in E9.5 *Mgat-1*$^{-}$*/Mgat-1*$^{-}$ embryos with the production of fore-, mid- and hindbrain regions, the branchial arches and myocardium. However, in the absence of complex N-linked oligosaccharides, embryos were approximately one-half to two-thirds the size of wild-type or heterozygous embryos (Figure 4A and data not shown). Moreover, E9.5 *Mgat-1*$^{-}$*/Mgat-1*$^{-}$ embryos exhibited only 20–22 somites prior to resorption as compared with E9.5 *Mgat-1*$^{+}$*/Mgat-1*$^{+}$ embryos that generally harbored 26 somites. Additionally, somites that formed in *Mgat-1*$^{-}$*/Mgat-1*$^{-}$ embryos were usually less well developed (data not shown). The overall morphology of *Mgat-1*$^{-}$*/Mgat-1*$^{-}$ embryos prior to resorption indicated that development proceeded to approximately E9.0, although viability may have continued until approximately E10.5. Heterozygous *Mgat-1*$^{+}$*/Mgat-1*$^{-}$ embryos appeared indistinguishable from those harboring functional *Mgat-1* genes at both alleles, regardless of the parental source of the mutant *Mgat-1* allele.

Loss of complex N-linked oligosaccharides did not appear to affect the differentiation of multiple cell types as judged by histology and the expression of cell type-specific proteins (Figure 4 and data not shown). In contrast, morphogenic processes were found to be impaired. Neural epithelial cells were present although neural folds were highly convoluted and fused to form a staggered suture line (Figure 4B–D and G). Nevertheless, neural epithelium in *Mgat-1*$^{-}$*/Mgat-1*$^{-}$ embryos appeared to exhibit an increase in mitotic events (Figure 4E and H).

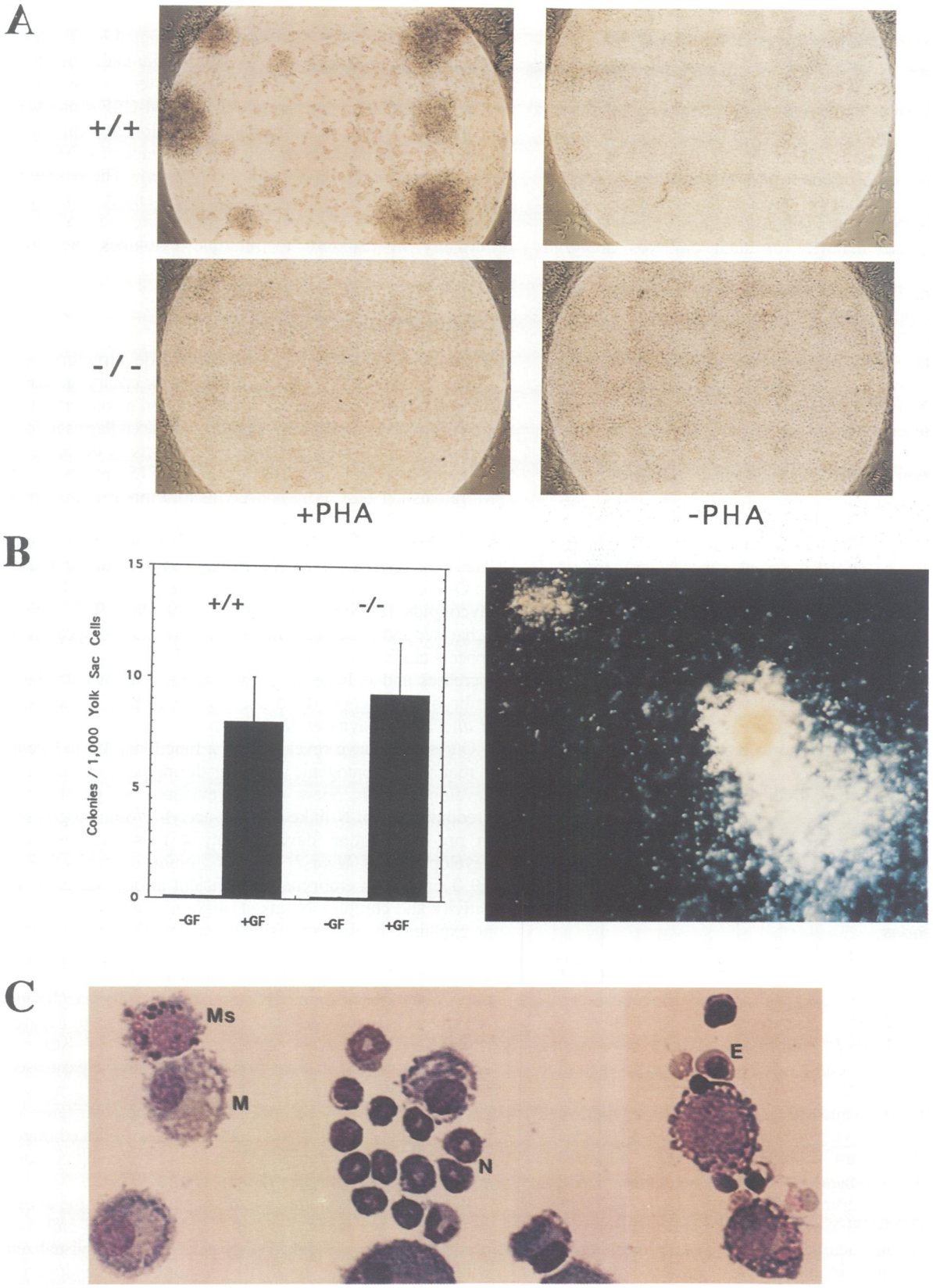

Fig. 6. Yolk sac E9.5 hemopoietic stem cells lacking GlcNAc-TI do not aggregate with PHA and respond normally in cytokine-mediated differentiation. (**A**) E9.5 yolk sac cells isolated from *Mgat-1*$^{+}$*/Mgat-1*$^{+}$ (+/+) or *Mgat-1*$^{-}$*/Mgat-1*$^{-}$ (−/−) embryos were cultured in the presence (+PHA) or absence (−PHA) of 20 μg/ml of L-PHA. (**B**, left) Frequency of hemopoietic colony formation with E9.5 yolk sac cells isolated from *Mgat-1*$^{+}$*/Mgat-1*$^{+}$ (+/+) or *Mgat-1*$^{-}$*/Mgat-1*$^{-}$ (−/−) embryos. Yolk sac cells were cultured in the absence (−GF) or presence (+GF) of a mixture of hemopoietic growth factors consisting of rSLF, GM-CSF, IL-3, Epo, MCSF-1 and IL-11. Hemopoietic colonies were visualized and quantitated after 8 days. (B, right) Colonies included burst-forming units that contained hemoglobin and represented erythroid differentiation. (**C**) Yolk sac derived hemopoietic cells isolated from an *Mgat-1*$^{-}$*/Mgat-1*$^{-}$ embryo after 6 days in culture in the presence of the above described cytokine mixture. Cell morphology and identification were assessed following May−Grünwald−Giemsa staining. Ms, mast cell; M, macrophage; N, neutrophil; E, nucleated erythrocyte.

Left–right asymmetry is frequently inverted in Mgat-1⁻/Mgat-1⁻ embryos

By E9.5, normal E9.5 mouse embryos have completed turning and display left–right body plan asymmetry with the tail coiled to the right side and a cardiac D loop (Tihen *et al.*, 1948). In contrast, E9.5 *Mgat-1⁻/Mgat-1⁻* embryos often failed to complete the turning process and frequently displayed an altered tail position that was oriented towards the left side of the embryo (Figure 4A and data not shown). Additionally, the majority of such embryos analyzed displayed an inverted heart loop structure (compare Figure 4F and I). These observations therefore revealed a *situs inversus* phenotype similar to that described following homozygous *iv* mutation which reverses left–right asymmetry in ~50% of mouse embryos (Layton, 1976). Complex N-linked oligosaccharide structures therefore play a crucial role in the formation of left–right asymmetry during mouse embryogenesis.

Vascularization is impaired in Mgat-1⁻/Mgat-1⁻ embryos

Hemopoiesis with the production of nucleated red blood cells is initiated at E7.0 in yolk sac tissue. By E9.5, normal embryos have developed a vascular system sufficient for blood cell circulation through arteries and veins. We observed that some E9.5 *Mgat-1⁻/Mgat-1⁻* embryos appeared anemic (Figure 4A) and many displayed accumulations of red blood cells in unexpected compartments, including the primitive head region and in proximity to the dorsal aorta and primary head vein (Figure 5A). These accumulations occurred within areas of dilated vasculature (Figure 5B). Vascular hypertrophy often included the embryonic heart (Figure 5A and data not shown). Although the presence of endothelial cell boundaries suggested that effective endothelial cell–cell junctions were present at E9.5, hemorrhages were observed by E10.5 (data not shown).

Hemopoiesis in the absence of complex N-linked oligosaccharides

Yolk sac-derived hemopoietic cells at E9.5 normally express complex N-linked oligosaccharides, as shown by L-PHA-induced cell aggregation (Figure 5A). In contrast, this multivalent lectin failed to aggregate yolk sac cells derived from *Mgat-1⁻/Mgat-1⁻* embryos as would be expected following loss of complex N-linked oligosaccharide structures (Figure 6A).

Significant growth and differentiation of hemopoietic cell types occurred following *in vitro* culture of yolk sac cells in semi-solid medium supplemented with a mixture of hemopoietic growth factors comprising steel factor (rSLF), interleukin-3 (IL-3), granulocyte-macrophage colony stimulating factor (GM-CSF), erythropoietin (Epo), macrophage colony stimulating factor-1, (MCSF-1) and interleukin-11 (IL-11). Remarkably, in the absence or presence of complex N-linked oligosaccharides, there were no differences in the frequency of colony-forming cells, the nature of the colonies formed, or in the cell number of resulting colonies (Figure 6B, left; and data not shown). In both instances large erythroid bursts that exhibited hemoglobin production were present (Figure 6B, right). Hemopoietic cell types that were produced in the absence of complex N-linked oligosaccharides included neutrophilic granulocytes, macrophages, nucleated erythrocytes and large cells with multi-lobed nuclei resembling megakaryocytes, as well as immature myeloid cells (Figure 6C and data not shown). Moreover, responses of yolk sac hemopoietic stem cells to GM-CSF alone was vigorous, resulting in the formation of colonies comprising relatively large numbers of cells at a frequency of 1/200 yolk sac cells over 12 days (data not shown). These results revealed that E9.5 *Mgat-1⁻/Mgat-1⁻* embryos contain hemopoietic progenitor cells that differentiate and proliferate normally in response to multiple cytokines including erythropoietin and GM-CSF.

Discussion

Stage-specific changes in oligosaccharide structures on glycoproteins normally occur during early embryogenesis. Pre-implantation and early post-implantation mouse embryos are rich in large fucose-containing poly-*N*-acetyllactosaminoglycans. Synthesis of these structures starts to decrease at E10 and reaches very low levels by E15 (reviewed in Muramatsu, 1992). Poly-*N*-acetyllactosaminoglycans carry the stage-specific embryonic antigen-1 (SSEA-1 or Le^x, Galβ1-4(Fucα1-3)GlcNAc) and other developmentally regulated oligosaccharide determinants. SSEA-1 can be found on O- and N-linked oligosaccharide structures as well as on glycolipids (Eggens *et al.*, 1989; Fukuda, 1990, 1992; Schachter and Brockhausen, 1992). This embryoglycan first appears at the 8-cell stage at the time when cell adhesiveness increases and is believed to be essential for morula-stage embryo compaction (Bird and Kimber, 1984; Fenderson *et al.*, 1984; Bayna *et al.*, 1989).

Our studies have revealed that a functional *Mgat-1* gene is required for ontogenic processes during post-implantation development. In view of the evidence suggesting the predominance of N-linked poly-*N*-acetyllactosaminoglycans in pre-implantation development, it is remarkable that development of *Mgat-1⁻/Mgat-1⁻* embryos proceeded to E9.0 since such embryos are deficient in both GlcNAc-TI activity and complex N-linked oligosaccharides. This may be explained by the expression of embryoglycans, including SSEA-1, on glycolipids and O-linked oligosaccharide structures. It is also possible that in the absence of N-linked poly-*N*-acetyllactosaminoglycans, specific oligosaccharide structures may be increased on other carrier molecules (Fukuda, 1990). Alternatively, a GlcNAc-TI isozyme encoded by a gene distinct from *Mgat-1* may be expressed at earlier stages of development. Although unlikely, embryogenesis to E9.0 may be dependent upon the persistence of paternally derived GlcNAc-TI and complex N-linked oligosaccharides that are transported between developing gametes across interstitial bridges (Braun *et al.*, 1989).

While additional studies can distinguish among the above possiblities, we have found that normal mouse embryos produce complex N-linked oligosaccharides, as visualized with PHA binding, by E7.0 on embryonic endoderm, mesoderm and ectoderm germ layers (unpublished data). Hence complex N-linked oligosaccharide synthesis begins well before lethality occurs in *Mgat-1⁻/Mgat-1⁻* embryos. It can be hypothesized that the absence of these structures is not detrimental to the embryo until specific ontogenic processes occur during post-implantation development at approximately E9.0. Our results also imply that complex N-linked oligosaccharides are functionally distinct from other

oligosaccharide structures. For example, it has been shown that expression of a virally encoded sialic acid-specific 9-*O*-acetylesterase in mouse embryos is lethal prior to the first mitotic division (Varki *et al.*, 1991). In that approach both N- and O-linked oligosaccharide structures would have been affected by the removal of terminal sialic acid determinants. In contrast to the lethal effect of homozygous *Mgat-1* gene inactivation in embryos, CHO cells that lack a functional *Mgat-1* homolog grow normally in tissue culture (Stanley *et al.*, 1975). These observations indicate that complex N-linked oligosaccharides encode specific roles and do not appear to be essential for cell viability.

Cellular differentiation and morphogenesis in the absence of complex N-linked oligosaccharides

Various differentiated cell types that have emerged by E9.5 in normal mouse embryos were also present in *Mgat-1*$^-$/*Mgat-1*$^-$ embryos, implying that cellular differentiation may occur unimpeded in the absence of complex N-linked oligosaccharides. Neural epithelial cells, myocardial tissue and hemopoietic cell types all appeared to differentiate normally, as judged by histology and the expression of cell type-specific proteins (Figures 4–6 and data not shown). Moreover, while yolk sac hemopoietic stem cells from wild-type embryos were found to express complex N-linked oligosaccharides, they did not require these structures for differentiation programs activated by binding to specific recombinant cytokines including IL-3, GM-CSF, and erythropoietin. While our results do not directly address the function of complex N-linked oligosaccharides on the cytokines themselves, the demonstration that *Mgat-1*$^-$/*Mgat-1*$^-$ embryos generated erythrocytes, macrophages and a variety of hemopoietic progenitor cells *in vivo* implied the production of functional hemopoietic cytokines.

Loss of GlcNAc-TI activity and complex N-linked oligosaccharide synthesis resulted in a significant reduction in embryo size by approximately one-half to two-thirds by E9.5. Additionally, the process by which opposing neural epithelial folds join and fuse in a linear manner was affected, resulting in a highly convoluted neural tube with an irregularly shaped suture line. Additionally, mitotic figures among neural epithelial cells in *Mgat-1*$^-$/*Mgat-1*$^-$ embryos indicated that cell proliferation may be enhanced in the absence of complex N-linked oligosaccharides. It is possible that the defect in neural tube formation may be secondary to a loss of growth control mediated by interactions between neural epithelial cells and adjacent mesenchymal tissue.

E9.5 *Mgat-1*$^-$/*Mgat-1*$^-$ embryos displayed abnormalities in the completion of turning, often with the tail oriented towards the left side. Moreover, heart loop structure was found to be inverted in a majority of such embryos. This *situs inversus* phenotype is more similar in frequency to that observed following homozygous *iv* gene mutation which reverses left–right asymmetry in ~50% of cases (Layton, 1976) and does not reflect the *inv* mutation which reverses left–right asymmetry in 100% of embryos (Yokoyama *et al.*, 1993). We can conclude that GlcNAc-TI activity, and the resulting production of complex N-linked oligosaccharide structures, modulates biological signals that control the establishment of left–right body plan asymmetry in mice and likely other mammals. As implied, our data provide evidence that such a regulatory molecule(s) resides in extracellular compartments as GlcNAc-TI activity specifically modifies secreted and cell-surface proteins. An extracellular origin for signals regulating left–right body plan asymmetry is further evident from studies of the extracellular matrix in *Xenopus laevis* embryos (Yost, 1992).

Embryonic lethality in the absence of a functional Mgat-1 allele

Although reasons for embryonic lethality among various gene-targeted mice are not often evident, *Mgat-1*$^-$/*Mgat-1*$^-$ mice consistently displayed abnormalities in vascularization at a time when a substantial increase in red blood cell-mediated tissue oxygenation normally occurs. In the absence of GlcNAc-TI activity, blood cell circulation was impaired as accumulations of nucleated red blood cells were commonly observed in regions including the primary head vein and dorsal aorta. These accumulations were surrounded by dilations of vascular endothelium indicating that complex N-linked oligosaccharides may be required to mediate proliferative signals among endothelial cells during blood vessel formation. It is also possible that the endothelial cell–cell junctions were formed inefficiently in the absence of complex N-linked oligosaccharides, thus leading to the multiple hemorrhages observed by E10.5. The defect observed in vascularization provides a plausible explanation as to why *Mgat-1*$^-$/*Mgat-1*$^-$ embryos die, although impairments in other processes may have contributed.

The phenotypes that we have observed may result from loss of oligosaccharide motifs that encode physiologic information, potentially regardless of the specific protein backbone. Alternatively, our results may be explained by the inactivation of specific proteins that require complex N-linked oligosaccharides. As is the case with studies of enzyme mutations, these proteins are not easily identified. For example, loss of specific kinase and phosphatase genes, as a result of either naturally occurring mutations or gene-targeting experiments, generates changes in phosphate levels on many cellular proteins that are thus potential phenotypic effectors (Appleby *et al.*, 1992; Imamoto and Soriano, 1993; Nada *et al.*, 1993; Shultz *et al.*, 1993). Nevertheless, it is obvious that important biological information can be gained from studying the consequences of such mutations. Moreover, glycosyltransferase function in embryogenesis and physiology can now be addressed by described methods of regulating gene ablation in specific cell and tissue types within embryos and adult mice (Orban *et al.*, 1992; Gu *et al.*, 1993; Marth, 1994). Such experiments should be of significant value as our studies support the view that complex N-linked oligosaccharides do not control cellular differentiation *per se*, but instead play critical roles in mammalian morphogenesis.

Materials and methods

Targeting vector construction and ES cell gene targeting

The *Mgat-1* gene was cloned from a genomic Balb/c library (Pownall *et al.*, 1992) and a targeting vector was constructed by insertion of pMC1neopolyA (Thomas and Capecchi, 1987) into the single protein-encoding exon of the *Mgat-1* gene. The targeting vector was linearized with *Sac*I and 20 μg DNA were electroporated into D3 ES cells (Doetschmann *et al.*, 1985). The D3 ES cell line was maintained on irradiated primary embryonic fibroblasts in DMEM supplemented with 15% fetal calf serum (FCS) (Hyclone), 0.1 mM non-essential amino acids, 1 mM sodium pyruvate, 100 mM L-glutamine, 0.1 mM β-mercaptoethanol, and 1000 U/ml leukemia inhibitory factor (Esgro, Gibco/BRL). Following electroporation ES cells were cultured

on 0.1% gelatinized tissue culture dishes with 125 μg/ml G418 (active concentration) added 24 h later. After 10–12 days, single colonies were isolated under a dissecting microscope, with half of each clone replated onto a 24-well tissue culture dish. The remaining half was analyzed in pools of 8 by PCR. Each pool was lysed in 100 μl lysis buffer (20 mM Tris–Cl pH 8.7, 50 mM KCl, 0.45% NP-40, 0.45% Tween-20, 0.01% gelatin and 100 μg/ml proteinase K) overnight at 55°C. Proteinase K was then inactivated by heating at 94°C for 10 min. Subsequently 15 μl of each sample was subjected to PCR in a final volume of 100 μl containing 10 mM Tris–HCl (pH 8.7), 50 mM KCl, 1.5 mM $MgCl_2$, 0.01% gelatin, 3 mM of each dNTP, 1 μg of each oligonucleotide primer and 25 U/ml Taq polymerase (Perkin-Elmer) for 40 cycles (60 s at 94°C, 90 s at 60°C and 2 min at 72°C). One Neo-specific (5′-GATTCGCAGCGCAT-CGCCTT) and one *Mgat-1*-specific primer (5′-GTGCACTAGAATGCCATTTG) were used that resulted in the amplification of a 1 kb fragment from the targeted *Mgat-1* allele. Single homologous recombinant ES cell clones were identified and the recombination event confirmed by genomic Southern blotting analyses as depicted in Figure 2A.

Generation of chimeric and mutant mice

Clones of 10–15 ES cells were microinjected into C57Bl/6J blastocysts derived from 3.5 day p.c. pregnant mice and implanted into the uteri of pseudopregnant albino ICR mice. The production of chimeric mice was demonstrated by the presence of agouti coat color patches. Chimeric males were obtained and mated with C57BL/6J females to generate heterozygous and homozygous offspring.

Genotype determination of embryos and mice by PCR and Southern blot analysis

The genotype of E9.5 embryos was determined with yolk sac cells by PCR, as described above, using the Neo-specific primer (see above) and two *Mgat-1*-specific primers (5′-GCTGCTTGGATAAGTTGTTGC and 5′-AGCTGCTTCTGCTAGTGTAC). These primers resulted in the amplification of a 0.8 kb fragment from the wild-type *Mgat-1* allele and a 0.6 kb (as well as a faint 1.9 kb) fragment from the mutated *Mgat-1* allele. For Southern blot analysis genomic DNA was isolated from ES cells, mouse tail tissue or primary embryonic fibroblasts derived from disaggregated E9.5 embryos and cultured in DMEM, 10% FCS, 100 mM L-glutamine and 0.1 mM β-mercaptoethanol. 5 μg of genomic DNA was digested with *Nsi*I and hybridized with the 0.49 kb *Kpn*I fragment (see Figure 2A) as previously described (Marth *et al.*, 1985).

Determination of GlcNAc-TI activity

Extracts for GlcNAc-TI assays were obtained by first washing E9.5 embryos in PBS, after removal of yolk sac tissue, and Dounce homogenizing at 4°C in 25 mM Tris–HCl (pH 6.1), 2% Triton X-100 (v/v), 0.02% sodium azide and 1 mM PMSF (phenylmethylsulfonylfluoride). Protein concentrations of extracts were determined with BCA protein assay reagent (Pierce). GlcNAc-TI was assayed (Vella *et al.*, 1984; Palcic *et al.*, 1988) using a synthesized substrate, Manα1-6(Manα1-3)Manβ-ocytl [Man_3-$C_{(8)}$], or a substrate derived from ovalbumin [Manα1-6(Manα1-3)Manα1-6](Manα-1-3)Manβ1-4GlcNAcβ1-4GlcNAc-Asn (Man_5-Asn) and product formation was assayed by adsorption to and elution from Sep-Pak C_{18} reversed phase cartridges or ConA–Sepharose. GlcNAc-TII was assayed as for GlcNAc-TI except that the substrate was Manα1-6(GlcNAcβ1-2Manα1-3)-Manβ-octyl.

Expression of complex N-linked oligosaccharides

Embryo extracts (see above) were delipidated and digested with Pronase (Narasimhan *et al.*, 1979, 1986; Grey *et al.*, 1982). The glycopeptide fraction was labeled by *N*-[^{3}H]acetylation and purified by gel filtration on Sephadex G-25 (40 cm × 1 cm). Radioactive glycopeptides were analyzed by fractionation on ConA–Sepharose (Pharmacia, 0.7 × 8 cm) or ricin (RCA-120)–agarose (Miles-Yeda, 0.5 × 15 cm) as previously described (Narasimhan *et al.*, 1986; Bierhuizen *et al.*, 1988). Material analyzed on ricin columns was first hydrolyzed with 2 M acetic acid at 100°C for 15 min to expose galactosyl residues by removal of sialic acid. ConA–Sepharose-adherent radioactive material which was eluted with 0.5 M α-methyl-D-glucopyranoside did not adhere to ConA–Sepharose after treatment with endo-*N*-acetylglucosaminidase H (Boehringer-Mannheim) at pH 6.0 for 16 h at 30°C and therefore contains high-mannose N-linked oligosaccharide structures. RCA-120–agarose-adherent material which was eluted with 0.1 M lactose contains tri- and tetra-antennary complex N-linked oligosaccharide structures with galactose residues at the non-reducing termini (Narasimhan *et al.*, 1986; Bierhuzen *et al.*, 1988).

Lectin binding analyses to nitrocellulose-bound glycoproteins

Samples of wild-type (++), heterozygous (+/−), and *Mgat-1*$^-$/*Mgat-1*$^-$ (−−) mouse E9.5 embryo extracts containing 22.5 μg of protein were electrophoresed on 10% SDS–polyacrylamide mini-gels (Laemmli, 1970), then transferred to nitrocellulose (Towbin *et al.*, 1979). Nitrocellulose blots were stained with Ponceau S then blocked and incubated with lectins and detection reagents using the buffer systems as described (Olmsted, 1981). Transfers were incubated with 0.5 mg/ml of either biotinylated *Ricinus communis* agglutinin I lectin (RCA I) or biotinylated ConA (Vector Laboratories) in the absence or presence of 1 M galactose or 1 M α-methyl D-mannoside, respectively, for 24 h. at 22°C. Bound lectins and biotinylated molecular weight standard proteins were detected using Vectastain ABC (Vector Laboratories). Lectin blots were developed using ECL (Amersham).

Histological analyses

After removal of yolk sac tissue, embryos were fixed in Bouins for 2 h, dehydrated in 70% ethanol and embedded in either paraffin or methacrylate. 5 μm sections were obtained and stained with hematoxylin–eosin.

PHA responses and colony forming assays

Yolk sacs of E9.5 embryos were isolated and incubated in 1 ml PBS, 20% FCS and 0.13% collagenase (Sigma) for 3–4 h at 37°C. Hank's salt solution containing 4% FCS was added and cell clumps were removed. The remaining cell suspension was washed twice and cell density was adjusted to 1×10^5/ml. For PHA binding, 1000 cells per well were cultured on Terrasaki plates in RPMI-1640 medium supplemented with 10% FCS (Intergen) in the absence or presence of 20 μg/ml of PHA (Pierce). The aggregation response was scored 3 h later.

Colony forming assays were accomplished by adding 500–1000 cells to 1 ml of RPMI-1640 medium, 10% FCS, 0.1 vol of 3% Bacto-Agar (Difco Laboratories, Detroit, MI) as described (Schrader *et al.*, 1981) in the presence or absence of a mixture of hemopoietic growth factors comprising recombinant murine steel factor (rSLF, 100 ng/ml), granulocyte macrophage colony stimulating factor (GM-CSF, 2×10^{-4} dilution of recombinant material), synthetic interleukin-3 (IL-3, 4 μg/ml), erythropoietin (0.01 U/ml), medium conditioned by L-cells (2% v/v) and medium conditioned by B9/IL-11 cells (5% v/v). Colonies were scored 8 days later using a dissecting microscope. Liquid cultures were generated in 96-well tissue culture plates (Falcon, Becton Dickinson, Mississauga, Ont.) in the presence of single or multiple hemopoietic growth factors. Cell smears were prepared using a Shandon Cytospin and were stained with May–Grünwald–Giemsa.

Acknowledgements

The authors thank Dr Jeffrey H.M.Charuk, Elena Merletti, Linda Trueman, Sheila Jalbert and Stephanie Buchanan for assistance with some of the experiments. Dr Janet Rossant provided the D3 ES cell line and Dr Hans Paulsen provided the Manα1-6(Manα1-3)Manβ-octyl reagent. This work was supported by grants from the National Cancer Institute of Canada and the NCE Genetics program to J.D.Marth, the Medical Research Council of Canada (MRC) to J.W.Schrader and by the Swiss National Research Foundation to M.Metzler. M.Sarkar and H.Schachter are supported by grants from the NCE Protein Engineering program and the MRC.

References

Appleby,M.W., Gross,J.A., Cooke,M.P., Levin,S.D., Qian,X. and Perlmutter,R.M. (1992) *Cell*, **70**, 751–763.

Bayna,E.M., Shaper,J.H. and Shur,B.D. (1988) *Cell*, **53**, 145–157.

Bierhuizen,M.F.A., Edzes,H.T., Schiphorst,W.E.C.M., van den Eijnden,D.H. and van Dijk,W. (1988) *Glycoconjugate J.*, **5**, 85–97.

Bird,J.M. and Kimber,S.J. (1984) *Dev. Biol.*, **104**, 449–460.

Bolscher,J.G.M., Van der Bijl,M.M.W., Neefjes,J.J., Hall,A., Smets,L.A. and Ploegh,H.L. (1988) *EMBO J.*, **7**, 3361–3368.

Braun,R.E., Behringer,R.R., Peschon,J.J., Brinster,R.L. and Palmiter,R.D. (1989) *Nature*, **337**, 373–376.

Brockhausen,I., Carver,J. and Schachter,H. (1988) *Biochem. Cell Biol.*, **66**, 1134–1151.

Dennis,J.W., Laferte,S., Waghorne,C., Breitman,M.L. and Kerbel,R.S. (1987) *Science*, **236**, 582–585.

Doetschman,T.C., Eistetter,H., Katz,M., Schmidt,W. and Kemler,R. (1985) *J. Embryol. Exp. Morphol.*, **87**, 27–45.

Eggens,I., Fenderson,B., Toyokuni,T. and Hakomori,S. (1989) *Biochem. Biophys. Res. Commun.*, **158**, 913–920.

Fenderson,B.A., Zahavi,U. and Hakomori,S. (1984) *J. Exp. Med.*, **160**, 1591–1596.

Fernandes,B., Sagman,U., Auger,M., Demetrio,M. and Dennis,J.W. (1991) *Cancer Res.*, **51**, 718–723.
Fukuda,M. (1992) In Fukuda,M. (ed.), *Cell Surface Carbohydrates and Cell Development*. CRC Press, Boca Raton, FL, pp. 127–159.
Fukuda,M.N. (1990) *Glycobiology*, **1**, 9–15.
Grey,A.A., Narasimhan,S., Brisson,J.-R., Schachter,H. and Carver,J.P. (1982) *Can. J. Biochem.*, **60**, 1123–1131.
Gu,H., Zou,Y.-R. and Rajewsky,K. (1993) *Cell*, **73**, 1155–1164.
Imamoto,A. and Soriano,P. (1993) *Cell*, **73**, 1117–1124.
Kornfeld,R. and Kornfeld,S. (1985) *Annu. Rev. Biochem.*, **54**, 631–664.
Kumar,R. and Stanley,P. (1989) *Mol. Cell. Biol.*, **9**, 5713–5717.
Kumar,R., Yang,J., Larsen,R.D. and Stanley,P. (1990) *Proc. Natl Acad. Sci. USA*, **87**, 9948–9952.
Kumar,R., Yang,J., Eddy,R.L., Byers,M.G., Shows,T.B. and Stanley,P. (1992) *Glycobiology*, **2**, 383–393.
Kukuruzinska,M.A., Bergh,M.L.E. and Jackson,B.J. (1987) *Annu. Rev. Biochem.*, **56**, 915–944.
Laemmli,U.K. (1970) *Nature*, **227**, 680–685.
Lasky,L.A. (1992) *Science*, **258**, 964–969.
Layton,W.M. (1976) *J. Hered.*, **67**, 336–338.
Marth,J.D. (1994) *Glycoconjugate J.*, **11**, in press.
Marth,J.D., Peet,R., Krebs,E.G. and Perlmutter,R.M. (1985) *Cell*, **43**, 393–404.
Möller,G., Reck,F., Paulsen,H., Kaur,K.J., Sarkar,M., Schachter,H. and Brockhausen,I. (1992) *Glycoconjugate J.*, **9**, 180–190.
Muramatsu,T. (1988) *Biochimie*, **70**, 1587–1596.
Muramatsu,T. (1992) In Fukuda,M. (ed.), *Cell Surface Carbohydrates and Cell Development*. CRC Press, Boca Raton, FL, pp. 239–256.
Nada,S., Yagi,T., Takeda,H., Tokunaga,T., Nakagawa,H., Ikawa,Y., Okada,M. and Aizawa,S. (1993) *Cell*, **73**, 1125–1135.
Narasimhan,S., Wilson,J.R., Martin,E. and Schachter,H. (1979) *Can. J. Biochem.*, **57**, 83–96.
Narasimhan,S., Freed,J.C. and Schachter,H. (1986) *Carbohydr. Res.*, **149**, 65–83.
Nishikawa,Y., Pegg,W., Paulsen,H. and Schachter,H. (1988) *J. Biol. Chem.*, **263**, 8270–8281.
Olmsted,J.B. (1981) *J. Biol. Chem.*, **256**, 11955–11957.
Orban,P.C., Chui,D. and Marth,J.D. (1992) *Proc. Natl Acad. Sci. USA*, **89**, 6861–6865.
Palcic,M.M., Heerze,L.D., Pierce,M. and Hindsgaul,O. (1988) *Glycoconjugate J.*, **5**, 49–63.
Passaniti,A. and Hart,G.W. (1990) *Cancer Res.*, **50**, 7261–7271.
Paulson,J.C. and Colley,K.J. (1989) *J. Biol. Chem.*, **264**, 17615–17618.
Pownall,S., Kozak,C.A., Schappert,K., Sarkar,M., Hull,E., Schachter,H. and Marth,J.D. (1992) *Genomics*, **12**, 699–704.
Sarkar,M., Hull,E., Nishikawa,Y., Simpson,R.J., Moritz,R.L., Dunn,R. and Schachter,H. (1991) *Proc. Natl Acad. Sci. USA*, **88**, 234–238.
Schachter,H. and Brockhausen,I. (1992) In Allen,H.J. and Kisailus,E.C. (eds), *Glycoconjugates. Composition, Structure and Function*. Marcel Dekker, New York, NY, pp. 263–332.
Schachter,H., Brockhausen,I. and Hull,E. (1989) *Methods Enzymol.*, **179**, 351–396.
Schrader,J.W., Lewis,S.J., Clark-Lewis,I. and Culvenor,J.G. (1981) *Proc. Natl Acad. Sci. USA*, **78**, 323–327.
Shultz,L.D., Schweitzer,P.A., Rajan,T.V., Yi,T., Ihle,J.N., Matthews,R.J., Thomas,M.L. and Beier,D.R. (1993) *Cell*, **73**, 1445–1454.
Stanley,P., Narasimhan,S., Siminovitch,L. and Schachter,H. (1975) *Proc. Natl Acad. Sci. USA*, **72**, 3323–3327.
Tanner,W. and Lehle,L. (1987) *Biochim. Biophys. Acta*, **906**, 81–99.
Thomas,K.R. and Capecchi,M.R. (1987) *Cell*, **51**, 503–512.
Tihen,J.A., Charles,D.R. and Sippel,T.O. (1948) *J. Hered.*, **39**, 29–31.
Towbin,H., Staehelin,T. and Gordon,J. (1979) *Proc. Natl Acad. Sci. USA*, **76**, 4350–4354.
Varki,A. (1993) *Glycobiology*, **3**, 97–130.
Varki,A., Hooshmand,F., Diaz,S., Varki,N.M. and Hedrick,S.M. (1991) *Cell*, **65**, 65–74.
Vella,G.J., Paulsen,H. and Schachter,H. (1984) *Can. J. Biochem. Cell. Biol.*, **62**, 409–417.
Yokoyama,T., Copeland,N.G., Jenkins,N.A., Montgomery,C.A., Elder,F.F.B. and Overbeek,P.A. (1993) *Science*, **260**, 679–682.
Yost,H.J. (1992) *Nature*, **357**, 158–161.

Received on December 2, 1993

Note added in proof

Another study disrupting the *Mgat-1* gene has been recently reported by Ioffe,E. and Stanley,P. (1994) *Proc. Natl Acad. Sci. USA*, **91**, 728–732.